

# Catalytic aquathermolysis of Shengli heavy crude oil with an amphiphilic cobalt catalyst

Yan-Bin Cao<sup>1,2</sup> · Long-Li Zhang<sup>1</sup> · Dao-Hong Xia<sup>1</sup>

Received: 15 December 2015 / Published online: 2 July 2016  
© The Author(s) 2016. This article is published with open access at Springerlink.com

**Abstract** An interfacially active cobalt complex, cobalt dodecylbenzenesulfonate, was synthesized. Elemental analysis, atomic absorption spectroscopy, Fourier transform infrared spectroscopy (FT-IR), thermogravimetric analysis, and surface/interfacial tension determination were performed to investigate the properties of the catalyst. Results showed that the synthesized catalyst showed active interfacial behavior, decreasing the surface tension and interfacial tension between heavy oil and liquid phase to below 30 and 1.5 mN/m, respectively. The catalyst was not thermally degraded at a temperature of 400 °C, indicating its high thermal stability. Catalytic performance of the catalyst was evaluated by carrying out aquathermolysis. The viscosity determination showed that the viscosity of the heavy oil decreased by 38 %. The average molecular weight, group compositions, and average molecular structure of various samples were analyzed using elemental analysis, FT-IR, electrospray ionization Fourier transform ion cyclotron resonance (ESI FT-ICR MS), and <sup>1</sup>H nuclear magnetic resonance. Results indicated that the catalyst could attack the sulfur- and O<sub>2</sub>-type heteroatomic compounds in asphaltene and resin, especially the compounds with aromatic structure, leading to a decrease in the molecular

weight and then the reduction in the viscosity of heavy oil. Therefore, the synthesized catalyst might find an application in catalytic aquathermolysis of heavy oil, especially for the high-aromaticity heavy oil with high oxygen content.

**Keywords** Interfacially active CoDBS · Catalytic aquathermolysis · Oxygen-contained groups · Heavy oil

## 1 Introduction

Although heavy oil is an important supplement to traditional crude oil, especially in Canada, Venezuela, and China, it is difficult to recover and transport due to its highly viscous character (Shah et al. 2010; Hart 2014; Santos et al. 2014; Zhao et al. 2014). Many techniques have been proposed to reduce its viscosity during production, transportation, and processing, such as oil/water soluble viscosity reducing agents, thermal recovery, thermolysis, aquathermolysis, and visbreaking. Viscosity reducing agents are usually polymers or surfactants. The viscosity of heavy oil will be reduced notably if it is heated to a relative high temperature of 150–200 °C. The high viscosity will return when it cools down because no chemical reaction occurred during the thermal recovery. Thermolysis, or thermal cracking, can rupture heavy oil molecules, such as asphaltenes and resins, resulting in an irreversible viscosity reduction. However, the reaction temperature for heavy oil thermal cracking is usually above 300 °C (Hyne et al. 1982; Clark et al. 1983, 1984, 1987; Clark and Hyne 1984), which is very difficult to reach under reservoir conditions.

Catalysts and water have been adopted in thermal cracking of heavy oil to lower the reaction temperature after Hyne's pioneering work and the process was named catalytic aquathermolysis (Hyne et al. 1982). After more than

✉ Dao-Hong Xia  
xiadh@upc.edu.cn

Long-Li Zhang  
llzhang@upc.edu.cn

<sup>1</sup> State Key Laboratory of Heavy Oil Processing, China University of Petroleum, Qingdao 266580, Shandong, China

<sup>2</sup> Research Institute of Petroleum Engineering and Technology, Shengli Oilfield Company, Sinopec, Dongying 257000, Shandong, China

30 years of research, many types of catalysts have been used. These catalysts can be classified into three groups: (1) inorganic solid particles, such as mineral particles, metal oxides, metal sulfides (Clark et al. 1988; K ok 2009); (2) water soluble metal salts, including nickel, vanadium, iron salts (Chen et al. 2008, 2009; Yi et al. 2009; Luo et al. 2011); and (3) oil soluble metal compounds, such as molybdenum oleate (Zhao et al. 2008; Yi et al. 2009; Jeon et al. 2011; Chao et al. 2012). More recently, catalysts with surface and interfacial activity have attracted researchers' attention. They are usually metal complex compounds with a catalytically active metal ion and amphiphilic ligands, such as aromatic sulfonic iron, molybdenum, and nickel (Chen et al. 2008, 2010; Wang et al. 2010; Chao et al. 2012). Because most of the cracking reactions take place at the water/oil interface, amphiphilic catalysts are expected to show better performance than other type of catalysts. Amphiphilic catalysts are apt to adsorb at the interface, thus decreasing the interfacial tension and increasing the degree of mixing of water and heavy oil. More importantly, active metal ions are also concentrated at the interface, which improves the catalytic performance.

In this paper, an amphiphilic cobalt complex catalyst was synthesized and applied to reduce the viscosity of Shengli heavy oil. The ligand is dodecylbenzenesulfonic acid (DBSA), which provides interfacial activity to the compound, and the active metal  $\text{Co}^{2+}$ . The catalyst was cobalt dodecylbenzenesulfonate, CoDBS. The catalytic aquathermolysis of heavy oil was carried out in a high pressure autoclave at 250 °C. The viscosities of the heavy crude oil and the cracked heavy oil samples were determined at both 80 and 50 °C after dehydration strictly to avoid the influence of wax, and/or the effect of dilution and emulsification of water. The changes of heavy oil compositions, SARA (saturate, aromatic, resin, and asphaltene) compositions, and average molecular structures were studied to investigate the mechanism of heavy oil viscosity reduction during catalytic aquathermolysis.

## 2 Experimental

### 2.1 Experimental material

In experiments, the heavy oil used was from the Shengli Oilfield, China, with a viscosity of 8960 mPa s at 80 °C and 167,400 mPa s at 50 °C.

Almost all of the chemicals used in the study were of analytical grade and purchased from the Sinopharm Chemical Reagent Co. Ltd. Dodecylbenzenesulfonic acid (DBSA) was provided by the Tokyo Chemical Industry Co. Ltd and its purity was above 90 %. All reagents were used as-received without further purification.

### 2.2 Synthesis of the active cobalt catalyst

About 120 mL of 0.1 mol/L cobalt nitrate ( $\text{Ni}(\text{NO}_3)_2$ ) solution was accurately measured and introduced into a flask and incubated at 60 °C for 15 min in an oil bath. A 1 mol/L NaOH solution was slowly added drop-by-drop to keep the pH value of this solution at 11. After stirring for 20 min, the solution became opaque and then was vacuum-filtered with a Whatman membrane. The precipitate was washed three times with deionized water and then added to another flask, to which 10 g of DBSA was added. The flask was heated in an oil bath at 100 °C for 4 h, while the solution was stirred at 800 rpm. After that, the product was extracted with chloroform, and the by-products or unreacted solids were removed via centrifugation. The product was separated from chloroform by vacuum distillation and then dried under vacuum at 80 °C for 24 h. The collected product was a light blue powder, which was the desired catalyst.

### 2.3 Catalyst characterization

The elemental contents of C, H, S, and Co of the synthesized catalyst were determined with an elemental analyzer (Vario EL III, Elementar), combined with an atomic absorption spectrometer (ContraAA 700, Analytik Jena), and the content of O was calculated by subtracting the content of all other elements. The molecular structure was also characterized qualitatively with a Fourier transform infrared spectrometer (Nicolet 6700, Thermo) after being mixed with KBr.

The surface activity and interfacial activity between heavy oil and the catalyst solution were measured with a surface tensiometer (EasyDyne, Kr uss) and a spinning drop interfacial tensiometer (TX 500C, CNG).

The catalyst stability was evaluated with a thermogravimetric analyzer (WCT-1D, Beijing Optical Instruments) coupled with a differential thermal analyzer (DTA) under  $\text{N}_2$  atmosphere. The temperature was increased to 600 °C at 20 °C/min.

### 2.4 Catalytic aquathermolysis of Shengli heavy oil

A total of 140 g of heavy oil, 60 g of water, and 0.28 g of catalyst (0.2 wt%, mass ratio of the catalyst to heavy oil) was added to an autoclave. The temperature was raised to 250 °C in less than 1 h and was kept at 250 °C for 24 h. Then the autoclave was cooled down to room temperature with cooling water in less than 10 min. After that, the mixture was taken out, and dehydrated by distillation below 120 °C. Over 95 % water was removed. Then the viscosity of the heavy oil after aquathermolysis was measured with a Brookfield DV-III viscometer at both 80 and

50 °C. In order to obtain accurate data, the torque was kept at 50 % during measurements. The aquathermolysis experiments of heavy oil were repeated at least 3 times, and the data were averaged.

## 2.5 Analysis of heavy oil samples

Fourier transform ion cyclotron resonance mass spectrometry (FT-ICR MS) is an effective technique for analyzing the molecular structure of complex hydrocarbon systems, such as heavy oil (Qian and Robbins 2001; Hughey et al. 2002). Combined with soft ionization methods, e.g., electrospray ionization (ESI), FT-ICR MS was applied to investigate catalytic aquathermolysis of heavy oil (Wu et al. 2005; Smith et al. 2008; Colati et al. 2013; Wang et al. 2013). 10 mg oil sample was firstly dissolved in 1 mL toluene, and then diluted with toluene/methanol (1:3, v/v) to yield a 0.2-mg/mL solution. After that, 15  $\mu$ L ammonium hydroxide (28 %) solution was added to the 1-mL oil sample solution. The solution was vortex-mixed before analysis. The MS analysis was carried out on a Bruker Apex-ultra FT-ICR mass spectrometer with a 9.4 T superconducting magnet. The diluted sample solution was injected at 180  $\mu$ L/h. The atmospheric pressure photo ionization source was purchased from Bruker Daltonics. Nitrogen was used as the drying and nebulizing gas. The nebulizing gas temperature was 200 °C. The nebulizing gas flow rate was 1.2 L/min, and the drying gas flow rate was 5.0 L/min. For ESI, the main operating parameters were emitter voltage, 4.0 kV; capillary column introduction voltage, 4.5 kV; and capillary column end voltage,  $-320$  V. Ions were accumulated for 0.01 s in a hexapole with a 2.4-V direct current (DC) voltage. The optimized mass for Q1 was 250 Da. The extraction period for ions from the hexapole to the ICR cell was set to 1.2 ms. The RF excitation was attenuated at 12.5 dB and used to excite ions over the range of 115–800 Da. Spectra comprising 4 M data points were collected. The signal-to-noise ratio was improved by summing 128 scan FT-ICR datasets.

Mass spectra were internally calibrated using an extended homologous alkylation series (molecular ions of aromatic hydrocarbons and thiophenes) of high relative abundance in a mixed heavy oil within the mass range of 300–1000 Da. Data analysis was performed using custom software and the procedure has been described in detail elsewhere (Shi et al. 2009). The compounds were characterized by class (numbers of N, O, and S heteroatoms), type [rings plus double bond equivalence (DBE)], and carbon number. Species and their isotopes with different DBE values and carbon number were searched within a set  $\pm 0.001$  Kendrick mass defect (KMD) tolerance (Hughey et al. 2001).

The saturate, aromatic, resin, and asphaltene (SARA) fractions of heavy oil samples before and after catalytic aquathermolysis were separated and determined using alumina column chromatography. The average molecular weights of oil samples, resins, and asphaltenes were determined by vapor pressure osmometry (VPO) in a toluene solution. The C, H, S, and N contents of resins and asphaltenes were measured with an elemental analyzer (Elementar Vario EL III). FT-IR spectra of the resins and asphaltenes were collected on a Nicolet 6700 Fourier transform infrared spectrometer. The samples were daubed on a KBr disk to obtain a thin film.  $^1\text{H}$  NMR spectra of resins and asphaltenes were recorded on a Bruker ARX400 spectrometer.  $\text{CDCl}_3$  was used as the solvent and TMS as the internal chemical shift standard.

## 2.6 Analysis of gas products

Gas products of heavy oil after catalytic aquathermolysis were analyzed by an Agilent 7890A gas chromatograph with an Abel column AB-5MS (60 m  $\times$  0.25 mm  $\times$  0.25  $\mu$ m) and a flame ionization detector. High purity nitrogen was used as carrier gas.

# 3 Results and discussion

## 3.1 Characterization of the synthesized catalyst

The FT-IR spectra of DBSA and the synthesized cobalt catalyst are shown in Fig. 1. The typical peaks of the benzenesulfonic acid group are the stretching vibration peak of O–H (907  $\text{cm}^{-1}$ ) and the stretching vibration peaks of sulfate S=O (1363, 1177, and 1129  $\text{cm}^{-1}$ ) in the DBSA spectrum. In the spectrum of the catalyst, the stretching vibration peak of O–H at 907  $\text{cm}^{-1}$  vanished, and the stretching vibration peaks of sulfate S=O also shifted to higher wave number due to the inductive effect of the cobalt atom. Therefore, the synthesized compound was cobalt dodecylbenzenesulfonate (CoSDB). The elemental analysis results proved the molecular structure and composition of the synthesized catalyst (Table 1). The elemental composition is consistent with the stoichiometric values. The slightly higher H and O contents of the experimental results compared to those expected theoretically might be due to water absorption during the sample preparation.

The surface tension of the CoDBS aqueous solution decreased to approximately 27 mN/m when the CoDBS concentration was 0.02 wt% (Fig. 2). The interfacial tension between the CoDBS aqueous solution and heavy oil was also measured by a spinning drop method. At a

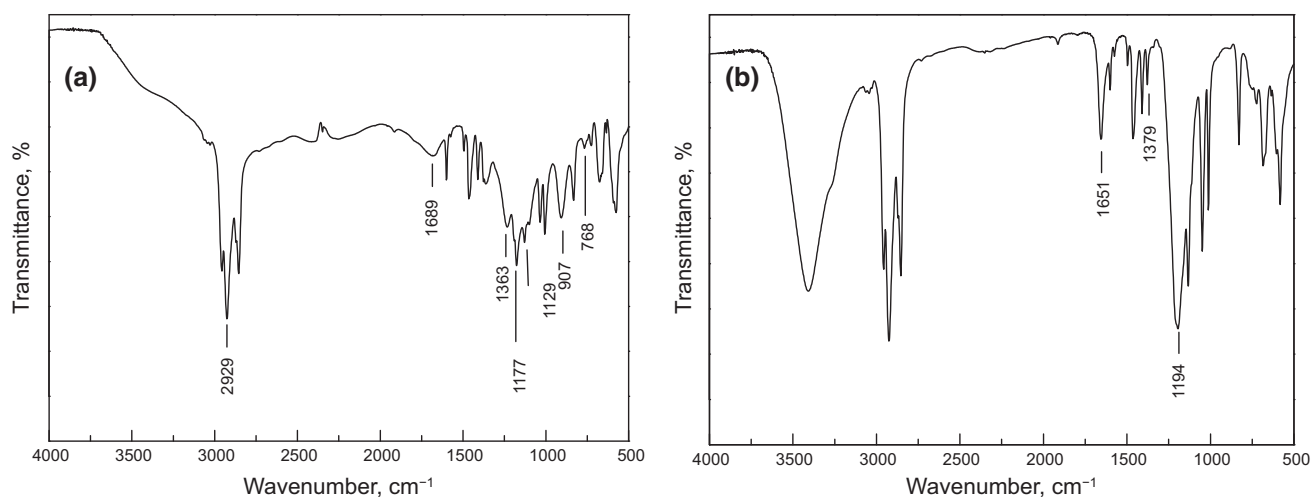


**Fig. 1** FT-IR spectra of DBSA (a) and CoDBS (b)

**Table 1** Elemental composition of the synthesized active cobalt catalyst

Elemental content	C, %	H, %	S, %	O, %	Co, %
Measured	57.37 ± 0.59	8.94 ± 0.17	8.59 ± 0.15	16.67 ± 0.18	8.43 ± 0.12
Theoretical	60.94 ± 0.44	8.18 ± 0.14	9.03 ± 0.13	13.54 ± 0.21	8.31 ± 0.13

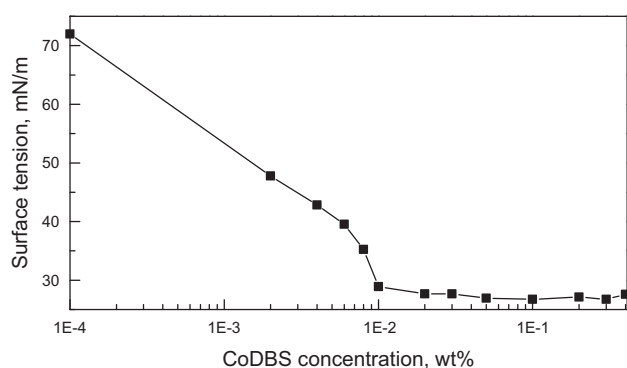


**Fig. 2** Surface tension of the synthesized CoDBS catalyst

concentration of 0.2 wt%, CoDBS could reduce the interfacial tension from about 20 mN/m to 0.7 mN/m. The interfacial activity of the CoDBS catalyst will benefit the emulsification of water and heavy oil. The better mixing and increased interfacial area between water and heavy oil might improve the cracking of asphaltene and resin in heavy oil, as asphaltene is partially surface active and apt to adsorb at the interface during aquathermolysis.

TGA-DTA (thermogravimetric analysis and differential thermal analysis) data of the synthesized catalyst are shown in Fig. 3. There is a significant weight loss and an exothermic peak at about 400 °C. This indicated that the catalyst does not decompose below 400 °C. That is to say, the CoDBS catalyst is thermally stable during the aquathermolysis process, usually below 300 °C.

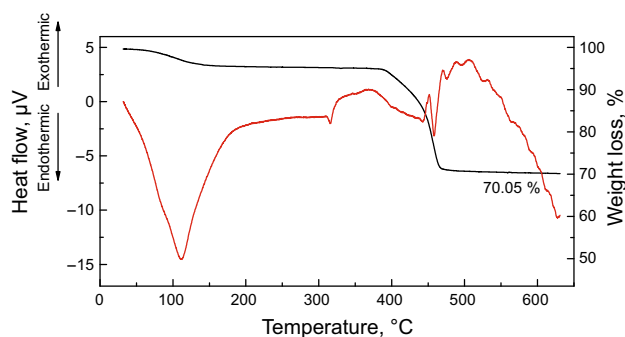


**Fig. 3** TGA (black line) and DTA (red line) curves of the CoDBS catalyst

### 3.2 Viscosity reduction and properties of the heavy oil after aquathermolysis

The viscosity of heavy oil was measured before and after catalytic aquathermolysis. The SARA compositions and average molecular weights of SARA components were also compared, as shown in Table 2. The viscosities of the heavy oil samples measured at 80 and 50 °C were reduced by 37.5 % and 57.5 %, respectively, after catalytic aquathermolysis. Because of the effect of microcrystalline wax, the reduction in oil viscosity measured at 80 °C was much lower than that measured at 50 °C. Compared with wax, large molecules, such as asphaltenes and resins, are the primary reason for the high viscosity of the heavy oil (Ghanavati et al. 2013). In order to elucidate the

**Table 2** Viscosity and SARA compositions of heavy oil samples

Sample	Heavy oils		Saturate		Aromatic		Resin		Asphaltene	
	Viscosity, mPa s	MW, g/mol	Content, wt% <sup>a</sup>	MW, g/mol <sup>b</sup>	Content, wt%	MW, g/mol	Content, wt%	MW, g/mol	Content, wt%	MW, g/mol
Heavy crude oil	8960 <sup>c</sup> 167,372 <sup>d</sup>	710	21.6	561.0	26.3	708.0	46.5	1454.0	5.5	10,031
Oil sample after aquathermolysis	5590 <sup>c</sup> 71,133 <sup>d</sup>	697	28.3	502.0	27.7	681.0	38.9	1503.0	5.1	9078

<sup>a</sup> Stands for the normalized weight percent of SARA

<sup>b</sup> Stands for the unit of average molecular weight of SARA

<sup>c</sup> Determined at 80 °C

<sup>d</sup> Determined at 50 °C

mechanism of viscosity reduction via catalytic aquathermolysis, the oil viscosity was measured at 80 °C unless otherwise specified. The oil viscosity decreased by 24.4 % at 80 °C in the control experiment without catalysts. The results proved that the synthesized catalyst can effectively reduce the viscosity of Shengli heavy oil.

The SARA analysis shows that asphaltene and resin contents decreased by 0.44 % and 7.65 % after aquathermolysis, respectively. In contrast, the contents of saturate and aromatic fractions of the oil sample increased by 6.69 % and 1.39 % after aquathermolysis. This indicates that the resin and asphaltene fractions were partly cracked into saturate and aromatic fractions during aquathermolysis. According to Table 2, the average molecular weights of heavy oil, saturates, aromatics, and asphaltenes decreased significantly after aquathermolysis, but the molecular weight of resins increased slightly in comparison with the original oil samples. It is known that a part of the resin cracks into saturates or aromatics, and meanwhile, the asphaltenes might crack into resins during thermolysis (Wang et al. 2009). The molecular weight of new resin transferred from asphaltene might be larger than that of the original resin, while the molecular weight of the later became smaller after cracking. Thus, the overall average molecular weight only changed slightly although the contents of resin decreased significantly. Moreover, the elemental compositions of various separated asphaltene and resin fractions were characterized and listed in Table 3. It is found that the S and N contents in the asphaltene fraction decreased accompanied by an increase in the two element contents in the resin fraction after aquathermolysis. The results indicate that part of high heteroatomic compounds in asphaltene fraction was transferred into resin.

High resolution MS was performed to study the changes of heteroatomic compounds in Shengli heavy oil before and after aquathermolysis. The results are shown in Figs. 4, 5, 6, 7, and 8 and Table 4. Because of the different ionizations of different compounds, the contents in Fig. 4 only

**Table 3** Elemental composition of the asphaltene and resin fractions

Elemental content, wt%	C	H	S	N
Asphaltenes	81.1	8.5	2.5	2.0
Asphaltenes after aquathermolysis	80.2	8.4	2.5	1.9
Resins	85.2	10.0	1.5	1.5
Resins after aquathermolysis	85.1	10.1	1.7	1.5

show the relative contents. For example, the sulfur compounds have a low ionization ratio and they also show low contents in Fig. 4. In the negative-ion mode of ESI FT-ICR MS, heteroatomic compounds including O<sub>2</sub>, N<sub>1</sub>, N<sub>1</sub>O<sub>2</sub>, O<sub>2</sub>S<sub>1</sub>, O<sub>3</sub>, O<sub>1</sub>, N<sub>1</sub>S<sub>1</sub>, N<sub>1</sub>O<sub>1</sub>, N<sub>2</sub>, N<sub>2</sub>O<sub>2</sub>S<sub>2</sub>, S<sub>1</sub>, and N<sub>1</sub>O<sub>2</sub>S<sub>2</sub> were detected in the heavy oil sample. After aquathermolysis, the contents of N<sub>2</sub>O<sub>2</sub>S<sub>2</sub>, S<sub>1</sub>, and N<sub>1</sub>O<sub>2</sub>S<sub>2</sub> decreased sharply, and were hardly detected. This indicates that the sulfur compounds are apt to crack during aquathermolysis because of the relatively small bond energy of C–S bonds, which also corresponds with the element analysis results. N<sub>1</sub>-, O<sub>1</sub>-, and O<sub>3</sub>-type contents increased after aquathermolysis while O<sub>2</sub> type decreased.

The type and content of N<sub>1</sub> compounds are shown in Fig. 5. The N<sub>1</sub> compounds in the negative-ion mode are nonbasic nitrogen compounds including pyrrole, benzopyrrole, carbazole, benzocarbazole, and dibenzocarbazole. Their DBE ranges from 9 to 16, and the carbon number is from 20 to 40 (C<sub>20</sub> to C<sub>40</sub>). After aquathermolysis, the DBE of the compounds ranged from 12 to 15, and the carbon number was from 20 to 40. Benzocarbazole-type compounds (DBE 12) and dibenzocarbazole (DBE 15) had the highest content. The N<sub>1</sub> compounds with DBE of 9–11 decreased. Almost no DBE 6 (benzopyrrole type) and DBE 3 (pyrrole type) compounds were detected.

According to the results of O<sub>1</sub> and O<sub>2</sub> compounds, the oxygen compounds in heavy crude oil are mainly phenolics and carboxylic acids. Because the carboxylic acid compounds are thermally instable, they tend to crack into

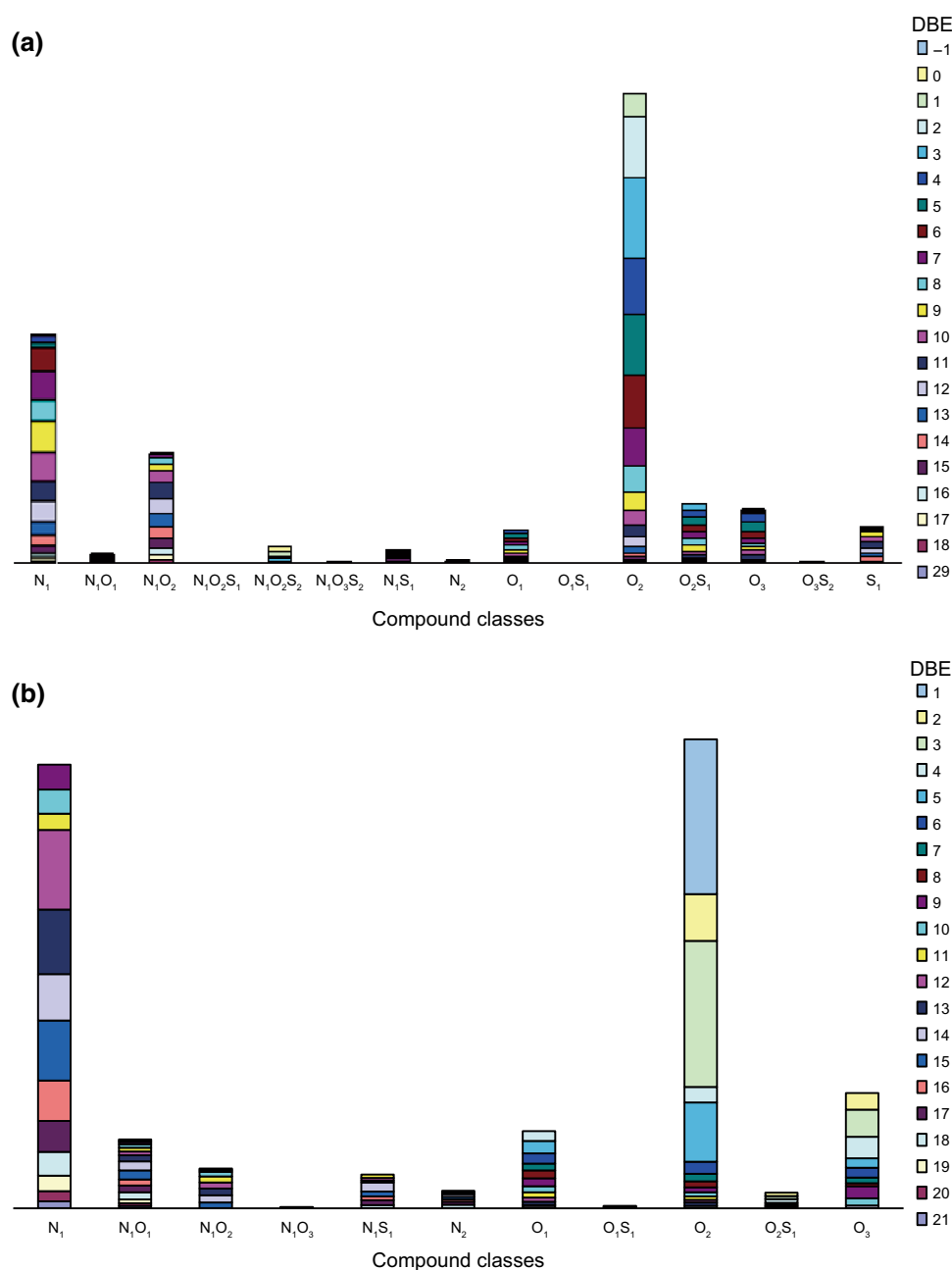


**Fig. 4** Relative contents of heteroatomic compounds in Shengli heavy oil by ESI FT-ICR MS (negative-ion mode). **a** Heavy crude oil. **b** Heavy oil after aquathermolysis

hydrocarbons and carbon dioxide during aquathermolysis. The phenolic compounds mainly include alkyl phenolic and alkyl benzophenolic (from benzophenolics to quadribenzophenolics) compounds. The  $O_1$  class of the negative-ion mode of ESI FT-ICR MS results is shown in Fig. 6. For heavy oil samples before and after aquathermolysis, the distributions of DBE and carbon number were continuous. DBE was from 4 to 9, while the carbon number was from 18 to 35 ( $C_{18}$  to  $C_{35}$ ). Since only the hydroxyl compounds can be ionized under the negative ESI mode,

and the minimal DBE was 4, it would be deduced that the  $O_1$  class compounds were mainly alkyl phenolics and their benzo-derivatives. The  $O_1$  class compounds are relatively stable, and their content did not change obviously after aquathermolysis.

As shown in Fig. 7, the DBE of  $O_2$  class compounds in the heavy oil sample was from 1 to 7, and their carbon numbers were from 16 to 35. After aquathermolysis, the DBE was from 1 to 3, and the carbon numbers were from 16 to 20. Furthermore, the contents also decreased

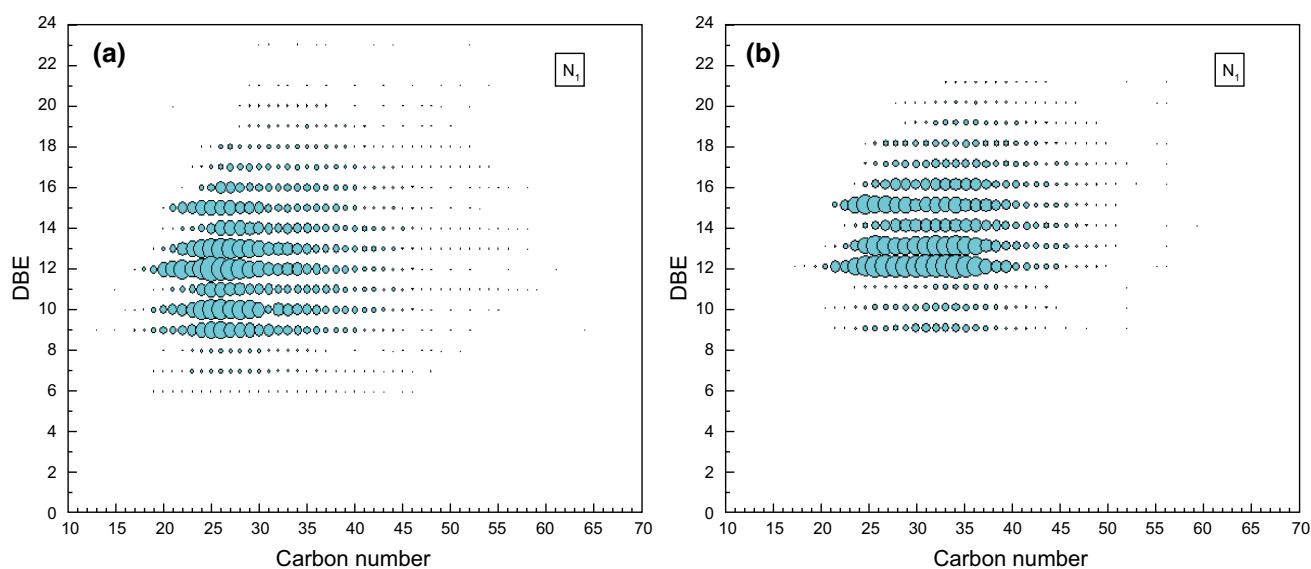


**Fig. 5** Types and distributions of  $N_1$  class compounds in Shengli heavy oil by ESI FT-ICR MS (negative-ion mode). **a** Heavy crude oil. **b** Heavy oil after aquathermolysis

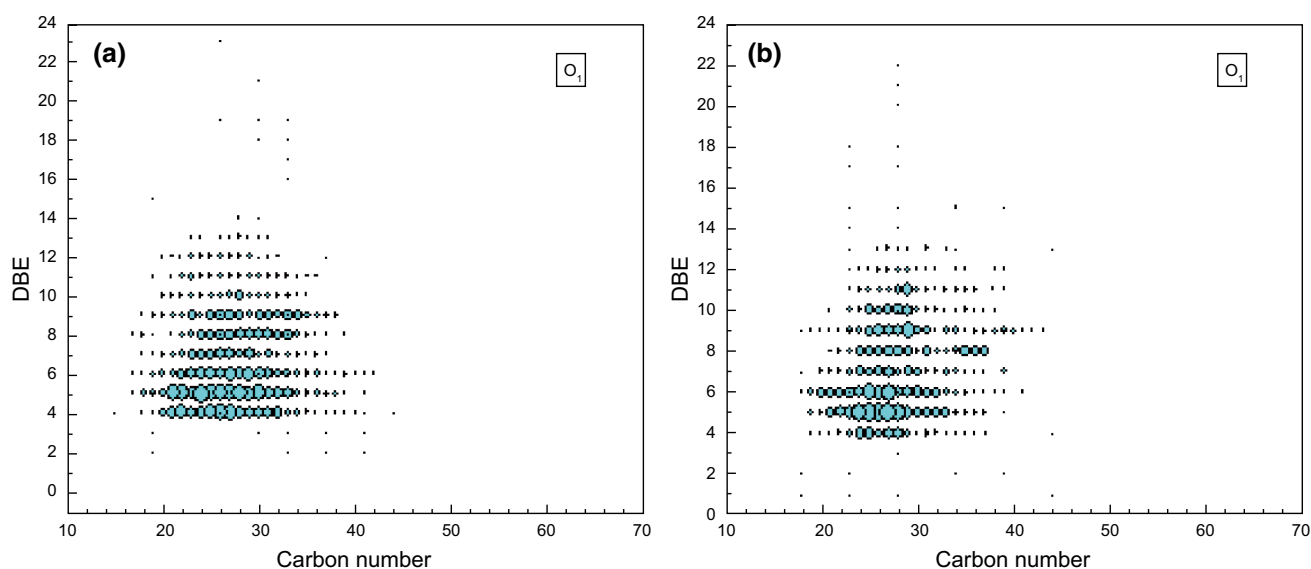


**Fig. 6** Types and distributions of  $O_1$  class compounds in Shengli heavy oil by ESI FT-ICR MS (negative-ion mode). **a** Heavy crude oil. **b** Heavy oil after aquathermolysis

obviously. The  $O_2$  class compounds of DBE 1 should be carboxylic acid compounds, and the DBE 2 should be naphthenic acids. The DBE 3–7 should be polyring naphthenic acids. Both carboxylic acids and naphthenic acids are active and easily cracked. As a result, the contents of  $O_2$  class compounds decreased significantly after catalytic reaction. The results of  $O_2S_1$  class compounds are shown in Fig. 8. Like  $O_2$  class compounds, their contents decreased noticeably. Their DBE was from 4 to 8, and the molecular structures should be thiophene rings fused with naphthenic

acids up to benzothiophene fused with dual ring naphthenic acids.

Other types of heteroatomic compounds are shown in Table 4, where  $N_1$ ,  $O_1$ ,  $O_2$ , and  $O_2S_1$  classes are identified in the negative-ion ESI FT-ICR MS spectrum. The sulfur compounds were easily cracked besides  $O_2$  class compounds for the low energy of C–S bond. Most of them were hardly detected in the heavy oil sample after aquathermolysis. For other heteroatomic compounds, their DBE and carbon number also decreased, which means that the large

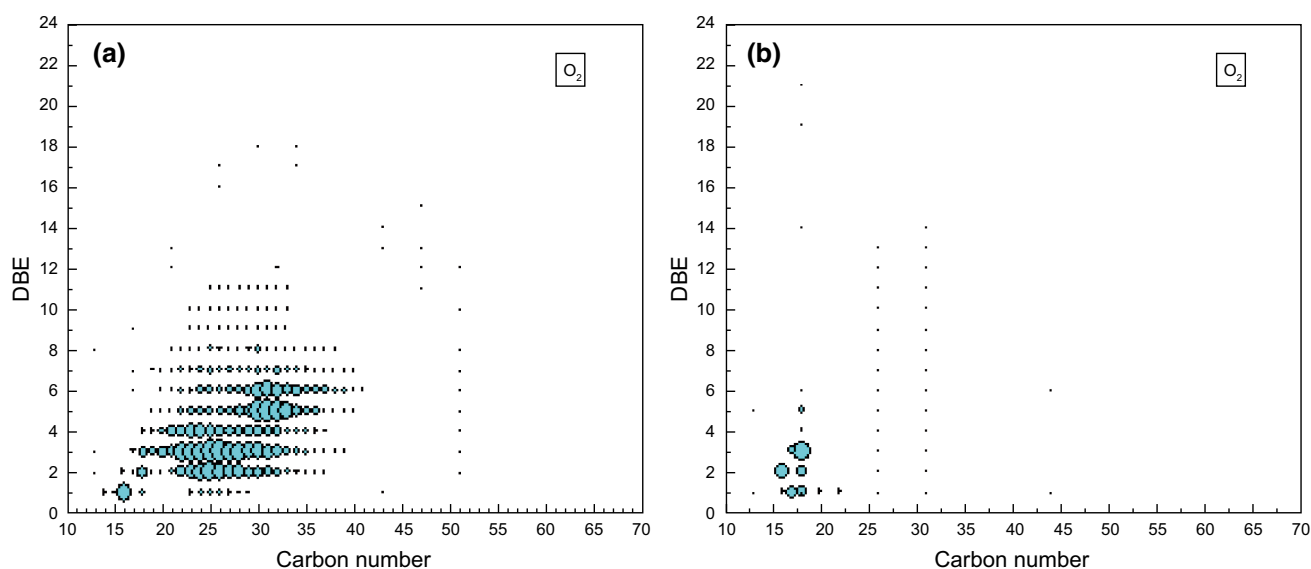


**Fig. 7** Types and distributions of  $O_2$  class compounds in Shengli heavy oil by ESI FT-ICR MS (negative-ion mode). **a** Heavy crude oil. **b** Heavy oil after aquathermolysis

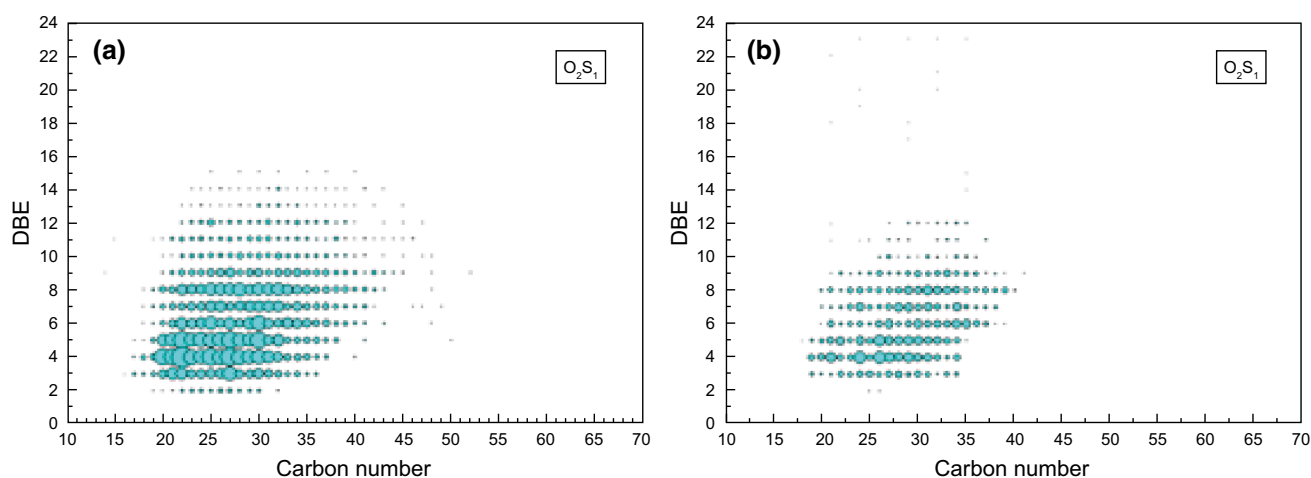


**Fig. 8** Types and distributions of  $O_2S_1$  class compounds in Shengli heavy oil by ESI FT-ICR MS (negative-ion mode). **a** Heavy crude oil. **b** Heavy oil after aquathermolysis

molecules cracked into relatively small molecules after aquathermolysis. The analytical results of gas products in Table 5 also show that  $H_2S$ ,  $CO_2$ ,  $H_2$ ,  $CO$ , and small hydrocarbons ( $C_1$ – $C_5$ ) were also detected, which also proved that the sulfur and oxygen heteroatomic compounds had been cracked.

### 3.3 Changes of the molecular structures of asphaltenes and resins

The above results show that the synthesized catalyst effectively reduced the viscosity of heavy oils during catalytic aquathermolysis, and the SARA analysis also shows

decreases in the asphaltene and resin contents. Since the asphaltene and resin are the high-molecular weight components, they might be the direct reason for the high viscosity of the heavy oil. It is necessary to study the change of the molecular structures of asphaltene and resin during the aquathermolysis process. FT-IR was used to characterize the ratio of groups to that of methyl groups,  $n_{CH_2}/n_{CH_3}$  of resin and asphaltene, which means the length of the aliphatic side chains, through Eq. (1) (Wang et al. 2009). According to the FT-IR spectra in Fig. 9, the calculated results are listed in Table 6. The  $n_{CH_2}/n_{CH_3}$  of asphaltene and resin fractions after aquathermolysis were smaller than those of the original ones. This indicates that



**Table 4** Various fractions of the heteroatomic compound groups in heavy oil samples before and after aquathermolysis (negative ions)

Heavy crude oil		Heavy oil after aquathermolysis		Summary of changes
Group	DBE and carbon number distribution	Group	DBE and carbon number distribution	
N <sub>1</sub>	9–15; C <sub>20</sub> –C <sub>35</sub>	N <sub>1</sub>	12–15; C <sub>20</sub> –C <sub>35</sub>	Some compounds decreased
N <sub>1</sub> O <sub>2</sub>	10–16; C <sub>20</sub> –C <sub>40</sub>	N <sub>1</sub> O <sub>2</sub>	10–15; C <sub>20</sub> –C <sub>40</sub>	Some compounds decreased
N <sub>1</sub> O <sub>1</sub>	13–18; C <sub>20</sub> –C <sub>35</sub>	N <sub>1</sub> O <sub>1</sub>	10–18; C <sub>20</sub> –C <sub>35</sub>	Parts of compounds decreased obviously
N <sub>1</sub> S <sub>1</sub>	11–17; C <sub>20</sub> –C <sub>35</sub>	N <sub>1</sub> S <sub>1</sub>	14–18; C <sub>20</sub> –C <sub>35</sub>	Some compounds decreased
N <sub>2</sub>	12–18; C <sub>20</sub> –C <sub>35</sub>	N <sub>2</sub>	12–18; C <sub>20</sub> –C <sub>35</sub>	Some compounds decreased
O <sub>2</sub> S <sub>1</sub>	3–9; C <sub>20</sub> –C <sub>35</sub>	O <sub>2</sub> S <sub>1</sub>	3–9; C <sub>20</sub> –C <sub>35</sub>	Parts of compounds decreased obviously
O <sub>1</sub> S <sub>1</sub>	6, 10; C <sub>24</sub> –C <sub>26</sub>	O <sub>1</sub> S <sub>1</sub>	6–8; C <sub>23</sub> –C <sub>27</sub>	Parts of compounds decreased obviously
O <sub>1</sub>	4–12; C <sub>18</sub> –C <sub>35</sub>	O <sub>1</sub>	4–11; C <sub>18</sub> –C <sub>35</sub>	Some compounds decreased
O <sub>2</sub>	1–8; C <sub>15</sub> –C <sub>35</sub>	O <sub>2</sub>	1–3; C <sub>15</sub> –C <sub>20</sub>	Parts of compounds decreased obviously
O <sub>3</sub>	4–11; C <sub>20</sub> –C <sub>35</sub>	O <sub>3</sub>	2–11; C <sub>18</sub> –C <sub>35</sub>	Parts of compounds decreased obviously
N <sub>1</sub> O <sub>3</sub> S <sub>2</sub>	2–4; C <sub>15</sub> –C <sub>30</sub>			Cracked totally
O <sub>3</sub> S <sub>2</sub>	2–6; C <sub>15</sub> –C <sub>30</sub>			Cracked totally
S <sub>1</sub>	6–15; C <sub>22</sub> –C <sub>50</sub>			Cracked totally
N <sub>1</sub> O <sub>2</sub> S <sub>1</sub>	11–13; C <sub>25</sub> –C <sub>30</sub>			Cracked totally
N <sub>1</sub> O <sub>2</sub> S <sub>2</sub>	4–8; C <sub>20</sub> –C <sub>35</sub>			Cracked totally

**Table 5** Gas product compositions of heavy oil after catalytic reaction

Gas products	H <sub>2</sub> S	H <sub>2</sub>	CO	CO <sub>2</sub>	CH <sub>4</sub>	C <sub>2</sub>	C <sub>3</sub>	C <sub>4</sub>	C <sub>5</sub>
Content, vol%	0.4	2.9	1.2	41.7	29.1	10.8	9.4	7.5	3.2

parts of the side chains were cracked during aquathermolysis. The side chains of resin were more apt to be cracked than those of asphaltene.

$$n_{CH_2}/n_{CH_3} = 2.93 A_{1460}/A_{1380} - 3.70 \quad (1)$$

where  $n_{CH_2}$  and  $n_{CH_3}$  are the number of methylene and methyl groups;  $A_{1460}$  and  $A_{1380}$  are the IR absorption intensity at 1460 and 1380  $cm^{-1}$ , respectively.

An improved Brown–Ladner method was adopted to calculate the molecular structures of resins and asphaltenes with the data of elemental analysis, average molecular weight, and <sup>1</sup>H-NMR (Suzuki et al. 1982; Ali et al. 1990; Strausz et al. 1992). The calculated results are listed in Table 7. The <sup>1</sup>H-NMR spectra of resins and asphaltenes are shown in Figs. 10 and 11. The aromaticity ( $f_A$ ) and

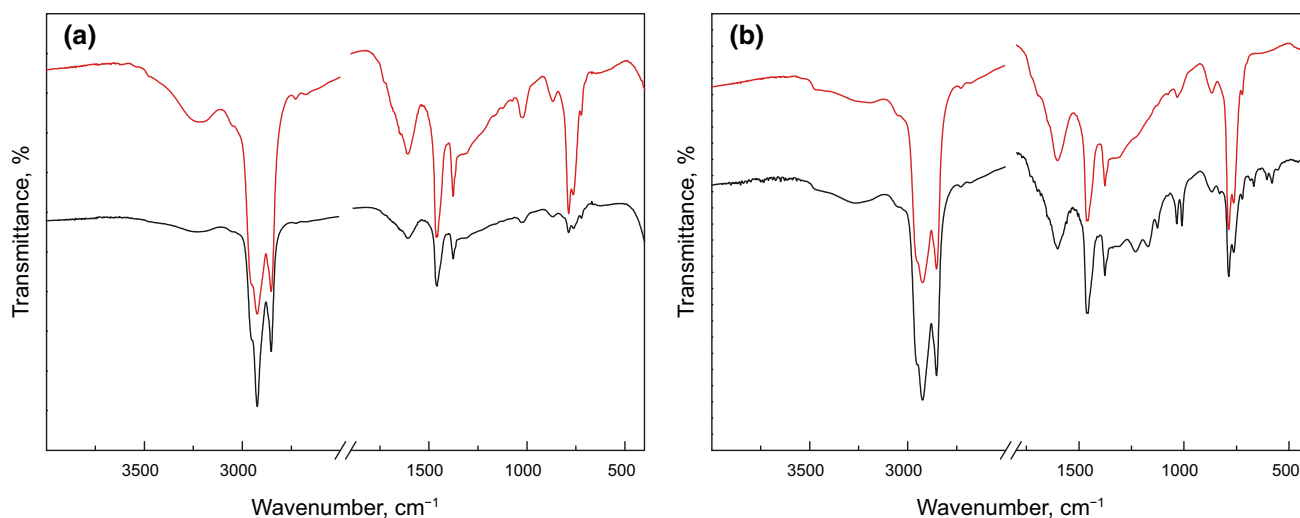


**Fig. 9** IR spectra of resins (a) and asphaltenes (b) extracted from heavy crude oil (red line) and heavy oil after aquathermolysis (black line)

**Table 6**  $n_{\text{CH}_2}/n_{\text{CH}_3}$  of asphaltenes and resins

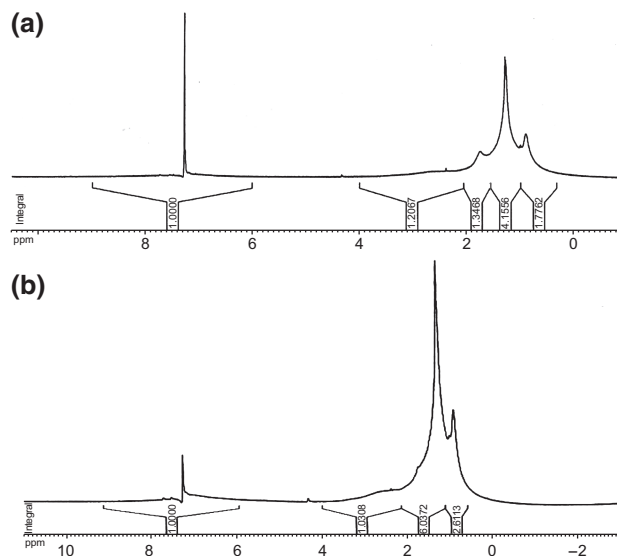
Sample	$n_{\text{CH}_2}/n_{\text{CH}_3}$
Heavy crude oil	
Asphaltene	0.212
Resin	0.644
Heavy oil after aquathermolysis	
Asphaltene	0.177
Resin	0.171

aromatic condensation index ( $H_{\text{AU}}/C_{\text{A}}$ ) of asphaltene and resin were calculated from Eqs. (2) and (3) (Liang 2000). The parameter  $H_{\text{AU}}/C_{\text{A}}$  establishes the relation between the average number of aromatic carbons and the number of carbon atoms probably incorporated into polycondensed structures of the asphaltenes and resins.

$$f_{\text{A}} = \frac{C/H - (H_{\alpha}^* + H_{\beta}^* + H_{\gamma}^*)/2H_{\text{T}}^*}{C/H} \quad (2)$$

$$\frac{H_{\text{AU}}}{C_{\text{AU}}} = \frac{H_{\text{A}}^*/H_{\text{T}}^* + H_{\alpha}^*/2H_{\text{T}}^*}{C/H - (H_{\alpha}^* + H_{\beta}^* + H_{\gamma}^*)/2H_{\text{T}}^*} \quad (3)$$

In Eqs. (2), (3), and Table 7,  $C/H$  is the atomic ratio of carbon to hydrogen, which is calculated from the elemental

**Fig. 10**  $^1\text{H}$  NMR spectra of asphaltene fraction extracted from heavy crude oil (a) and heavy oil after aquathermolysis (b)

analysis data.  $H_{\text{A}}^*$  refers to the relative content of aromatic hydrogens;  $H_{\alpha}^*$ ,  $H_{\beta}^*$ , and  $H_{\gamma}^*$  refer to relative content of hydrogens which are in  $\alpha$ ,  $\beta$ , and  $\gamma$  positions relative to aromatic rings:  $H_{\text{T}}^* = H_{\text{A}}^* + H_{\alpha}^* + H_{\beta}^* + H_{\gamma}^*$ .  $C$ ,  $C_{\text{A}}$ ,  $C_{\text{N}}$ , and

**Table 7** Average structure parameters of resin and asphaltene fractions extracted from heavy oil before and after aquathermolysis

Sample	Asphaltene		Resin	
	Heavy crude oil	Heavy oil after aquathermolysis	Heavy crude oil	Heavy oil after aquathermolysis
MW, g/mol	10,031	9078	1454	1403
C content, wt%	81.1	80.2	85.2	85.1
H content, wt%	8.5	8.4	10.0	10.1
$C/H$	0.796	0.791	0.707	0.699
Relative content, %				
$H_{\text{A}}^*$	10.54	6.49	7.25	6.88
$H_{\alpha}^*$	12.72	11.43	15.96	15.48
$H_{\beta}^*$	58.01	58.24	60.40	60.70
$H_{\gamma}^*$	18.73	23.84	16.39	16.95
$H_{\text{AU}}/C_{\text{A}}$	0.48	0.37	0.61	0.61
$R$	106.6	101.8	13.8	13.9
$R_{\text{A}}$	74.6	62.3	8.5	8.5
$R_{\text{N}}$	32.0	39.6	5.3	5.3
$C$	678.2	606.4	103.2	106.6
$C_{\text{A}}$	300.2	251.0	36.1	36.2
$C_{\text{N}}$	128.1	158.3	21.1	21.4
$C_{\text{P}}$	249.9	197.1	46.1	49.1
$f_{\text{A}}$	0.44	0.41	0.35	0.34
$f_{\text{N}}$	0.19	0.26	0.20	0.20
$f_{\text{P}}$	0.37	0.33	0.45	0.46

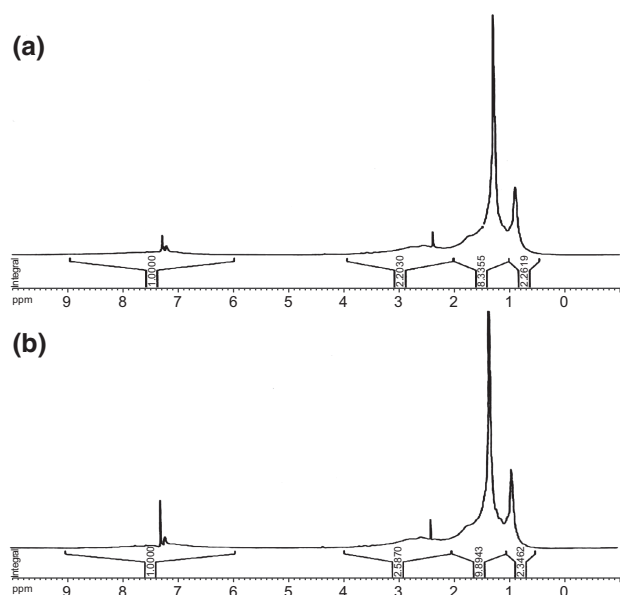


**Fig. 11**  $^1\text{H}$  NMR spectra of resin fraction extracted from heavy crude oil (a) and heavy oil after aquathermolysis (b)

$C_P$  are the total carbon number, aromatic carbon number, naphthenic carbon number, and paraffinic carbon number, respectively.  $R$  is the total number of rings;  $R_A$  is the number of aromatic rings; and  $R_N$  is the number of naphthenic rings.  $f_A$  is the ratio of the number of aromatic carbons to the total number of carbons;  $f_N$  is the ratio of the number of naphthenic carbons to the total number of carbons; and  $f_P$  is the ratio of the number of paraffinic carbons to the total number of carbons. The higher the  $H_{AU}/C_A$  ratio, the lower the aromatic condensation degree.

For asphaltene, both  $f_A$  and  $H_{AU}/C_A$  decreased after catalytic aquathermolysis. The reduction in aromaticity could be attributed to the rupture of polyring structures after the removal of heteroatoms or the hydrogenation of unsaturated groups, while the increase in the aromatic condensation degree might originate from the aggregation of aromatic units after the loss of side chains. For resin, the  $H/C$ ,  $f_A$  and  $H_{AU}/C_A$  changed slightly after catalytic aquathermolysis, almost the same as those of the crude resin. This is consistent with the previous results that the content of the resin changed much more but its molecular weight remained the same. It seems that during the aquathermolysis, the side chains of asphaltene might be more easily cracked than the side chains of resin, and parts of asphaltene might be transferred to resin after cracking.

The detailed structures of asphaltene and resin are also shown in Table 7. The average molecular structure of asphaltene changed significantly after aquathermolysis, while the resin remained ostensibly unchanged. Almost all the parameters of asphaltene, such as  $R_T$ ,  $R_A$ ,  $C_T$ ,  $C_A$ , and  $C_P$ , decreased after aquathermolysis. The smaller  $R_T$  and

$C_T$  of asphaltene proved that the cracking and ring-opening reactions occurred during aquathermolysis. The increased  $R_N$  and  $C_N$  also indicated that the aromatic rings were opened by hydrogenation. The decreased  $H_{AU}/C_A$  and increased  $f_N$  also indicated the lower aromatic condensation degree of the asphaltene after aquathermolysis. The changes of  $C_P$  and  $f_P$  further illustrated that the alkyl side chains were cracked off relatively easily over the catalyst. All these changes in the molecular structures of asphaltene benefited viscosity reduction and partially improved the quality of heavy oil. The changes of resin were more complicated than asphaltene. After aquathermolysis, part of the original resin was cracked into relatively small molecules, leading to a decrease in the average molecular weight, aromatic, and naphthenic ring numbers of the resin. Meanwhile, part of the cracked asphaltenes were of lower molecular weight and hence classified into resin fraction. After catalytic aquathermolysis, the resins might be of higher molecular weight, aromatic, and naphthenic ring numbers than the original resin. Therefore, the newly formed resin fraction had almost the same average molecular structure parameters compared with that of the original resin fraction.

In general, the catalytic aquathermolysis had more influence on the structure of the asphaltene than that of the resin. This is because the heteroatomic compounds, especially the sulfur and oxygen heteroatomic compounds, are usually found in the asphaltene fraction, where the bond energy of the C–S and C–O is lower than that of the C–C in every fractions. Therefore, the weak bonds are easier to crack by the catalyst during catalytic aquathermolysis and hence the high macromolecule content in asphaltene and resin fractions reduced. Moreover, asphaltenes are interfacially active compounds, and tend to adsorb at the water/oil interface. The addition of catalyst could reduce the interfacial tension force and improve the mixing of water and heavy oil, and meanwhile, the active metals, cobalt ions, were also concentrated at the interface. More importantly,  $\text{H}_2\text{O}$  would act as an H-donor in the catalytic reaction, where its role was same as that in heavy oil hydrotreatment. Therefore, the asphaltene could be cracked more easily.

## 4 Conclusion

In summary, we synthesized a complex cobalt compound with interfacial activity, cobalt dodecylbenzenesulfonate (CoDBS). It was thermally stable and suitable to be used as the catalyst in the catalytic aquathermolysis of heavy oil. The viscosity of heavy oil was significantly reduced after aquathermolysis. According to the SARA analysis and ESI FT-ICR MS results, the content of asphaltene and resin

reduced as a result of cracking of sulfur- and O<sub>2</sub>-type heteroatomic compounds. The catalyst would cause more changes of the aromatic structures in asphaltene according to the NMR results. The interfacially active complex cobalt compound catalyst is suitable for heavy oil viscosity reduction, especially for heavy oils of high-aromaticity and high oxygen content.

**Acknowledgments** The authors acknowledge the financial support from the Key Programs of Science and Technology of SINPOEC (Grant No. P11093).

**Open Access** This article is distributed under the terms of the Creative Commons Attribution 4.0 International License (<http://creativecommons.org/licenses/by/4.0/>), which permits unrestricted use, distribution, and reproduction in any medium, provided you give appropriate credit to the original author(s) and the source, provide a link to the Creative Commons license, and indicate if changes were made.

## References

- Ali LH, Al-Ghannam KA, Al-Rawi JM, et al. Chemical structure of asphaltenes in heavy crude oils investigated by NMR. *Fuel*. 1990;69(4):519–21. doi:10.1016/0016-2361(90)90326-L.
- Chao K, Chen YL, Li J, et al. Upgrading and visbreaking of super-heavy oil by catalytic aquathermolysis with aromatic sulfonic copper. *Fuel Process Technol*. 2012;104:174–80. doi:10.1016/j.fuproc.2012.05.010.
- Chen YL, He J, Wang YQ, et al. GC-MS used in study on the mechanism of the viscosity reduction of heavy oil through aquathermolysis catalyzed by aromatic sulfonic H<sub>3</sub>PMo<sub>12</sub>O<sub>40</sub>. *Energy*. 2010;35(8):3454–60. doi:10.1016/j.energy.2010.04.041.
- Chen YL, Wang YQ, Lu JY, et al. The viscosity reduction of nano-keggin-K<sub>3</sub>PMo<sub>12</sub>O<sub>40</sub> in catalytic aquathermolysis of heavy oil. *Fuel*. 2009;88(8):1426–34. doi:10.1016/j.fuel.2009.03.011.
- Chen YL, Wang YQ, Wu C, et al. Laboratory experiments and field tests of an amphiphilic metallic chelate for catalytic aquathermolysis of heavy oil. *Energy Fuels*. 2008;22(3):1502–8. doi:10.1021/ef800136.
- Clark PD, Dowling NI, Hyne JB, et al. The chemistry of organosulphur compound types occurring in heavy oils: 4. the high-temperature reaction of thiophene and tetrahydrothiophene with aqueous solutions of aluminium and first-row transition-metal cations. *Fuel*. 1987;66(10):1353–7. doi:10.1016/0016-2361(87)9018-5.
- Clark PD, Hyne JB. Chemistry of organosulphur compound types occurring in heavy oil sands: 3. reaction of thiophene and tetrahydrothiophene with vanadyl and nickel salts. *Fuel*. 1984;63(12):1649–54. doi:10.1016/0016-2361(84)90094-2.
- Clark PD, Hyne JB, Tyrer JD. Chemistry of organosulphur compound types occurring in heavy oil sands: 1. high temperature hydrolysis and thermolysis of tetrahydrothiophene in relation to steam stimulation processes. *Fuel*. 1983;62(8):959–62. doi:10.1016/0016-2361(83)90170-9.
- Clark PD, Hyne JB, Tyrer JD. Some chemistry of organosulphur compound types occurring in heavy oil sands: 2. influence of pH on the high temperature hydrolysis of tetrahydrothiophene and thiophene. *Fuel*. 1984;63(1):125–8. doi:10.1016/0016-2361(84)90266-7.
- Clark PD, Lesage KL, Tsang TG, et al. Reactions of benzo[b]thiophene with aqueous metal species: their influence on the production and processing of heavy oils. *Energy Fuels*. 1988;2(4):578–81. doi:10.1021/ef00010a027.
- Colati KA, Dalmaschio GP, Castro EVR, et al. Monitoring the liquid/liquid extraction of naphthenic acids in Brazilian crude oil using electrospray ionization FT-ICR mass spectrometry (ESI FT-ICR MS). *Fuel*. 2013;108:647–55. doi:10.1016/j.fuel.2013.02.007.
- Ghanavati M, Shojaei MJ, Ahamd RSR, et al. Effects of asphaltene content and temperature on viscosity of Iranian heavy crude oil: experimental and modeling study. *Energy Fuels*. 2013;27(12):7217–32. doi:10.1021/ef400776h.
- Hart A. A review of technologies for transporting heavy crude oil and bitumen via pipelines. *J Pet Explor Prod Technol*. 2014;4(3):327–36. doi:10.1007/s13202-013-0086-6.
- Hughey CA, Hendrickson CL, Rodgers RP, et al. Kendrick mass defect spectrum: a compact visual analysis for ultrahigh-resolution broadband mass spectra. *Anal Chem*. 2001;73(19):4676–81. doi:10.102/ac010560w.
- Hughey CA, Rodgers RP, Marshall AG, et al. Identification of acidic NSO compounds in crude oils of different geochemical origins by negative ion electrospray Fourier transform ion cyclotron resonance mass spectrometry. *Org Geochem*. 2002;33(7):743–59. doi:10.1016/S0146-6380(02)00038-4.
- Hyne JB, Clark PD, Clarke RA, et al. Aquathermolysis of heavy oils. *Rev Tec Intevp*. 1982;2(2):87–94.
- Jeon SG, Na JG, Ko CH, et al. Preparation and application of an oil-soluble CoMo bimetallic catalyst for the hydrocracking of oil sands bitumen. *Energy Fuels*. 2011;25(10):4256–60. doi:10.1021/ef200703t.
- Kök M. Influence of reservoir rock composition on the combustion kinetics of crude oil. *J Therm Anal Calorim*. 2009;97(2):397–401. doi:10.1007/s10973-008-9636-4.
- Liang W. Heavy oil chemistry. Beijing: China University of Petroleum Publishing House; 2000 (in Chinese).
- Luo H, Deng WN, Gao JJ, et al. Dispersion of water-soluble catalyst and its influence on the slurry-phase hydrocracking of residue. *Energy Fuels*. 2011;25(3):1161–7. doi:10.1021/ef014378.
- Qian KN, Robbins WK. Resolution and identification of elemental compositions for more than 3000 crude acids in heavy petroleum by negative-ion microelectrospray high-field Fourier transform ion cyclotron resonance mass spectrometry. *Energy Fuels*. 2001;15(6):1505–11. doi:10.1021/ef010111z.
- Santos RG, Loh W, Bannwart AC, et al. An overview of heavy oil properties and its recovery and transportation methods. *Braz J Chem Eng*. 2014;31(3):571–90. doi:10.1059/0104-6632.
- Shah AR, Fishwick R, Wood J, et al. A review of novel techniques for heavy oil and bitumen extraction and upgrading. *Energy Environ Sci*. 2010;3(6):700–14. doi:10.1039/B918960B.
- Shi Q, Xu CM, Zhao SQ, et al. Characterization of basic nitrogen species in coker gas oils by positive-ion electrospray ionization Fourier transform ion cyclotron resonance mass spectrometry. *Energy Fuels*. 2009;24(1):563–9. doi:10.1021/ef9008983.
- Smith DF, Schaub TM, Kim S, et al. Characterization of acidic species in Athabasca bitumen and bitumen heavy vacuum gas oil by negative-ion ESI FT-ICR MS with and without acid-ion exchange resin prefractionation. *Energy Fuels*. 2008;22(4):2372–8. doi:10.1021/ef8000345.
- Strausz OP, Mojelsky TW, Lown EM, et al. The molecular structure of asphaltene: an unfolding story. *Fuel*. 1992;71(12):1355–63. doi:10.1016/0016-2361(92)90206-4.
- Suzuki T, Itoh M, Takegami Y, et al. Chemical structure of tar-sand bitumens by <sup>13</sup>C and <sup>1</sup>H n.m.r. spectroscopic methods. *Fuel*. 1982;61(5):402–10. doi:10.1016/0016-2361(82)90062-x.
- Wang JQ, Li C, Zhang LL, et al. Phase separation and colloidal stability change of Karamay residue oil during thermal reaction. *Energy Fuels*. 2009;23(6):3002–7. doi:10.1021/ef801149q.

- Wang LT, He C, Zhang YH, et al. Characterization of acidic compounds in heavy petroleum resid by fractionation and negative-ion electrospray ionization Fourier transform ion cyclotron resonance mass spectrometry analysis. *Energy Fuels*. 2013;27(8):4555–63. doi:10.1021/ef400459m.
- Wang YQ, Chen YL, He J, et al. Mechanism of catalytic aquathermolysis: influences on heavy oil by two types of efficient catalytic ions: Fe<sup>3+</sup> and Mo<sup>6+</sup>. *Energy Fuels*. 2010;24(3):1502–10. doi:10.1021/ef901139k.
- Wu W, Song FR, Yan CY, et al. Structural analyses of protoberberine alkaloids in medicine herbs by using ESI-FT-ICR-MS and HPLC-ESI-MS<sup>n</sup>. *J Pharm Biomed Anal*. 2005;37(3):437–46. doi:10.1016/j.pba.2004.11.026.
- Yi YF, Li SY, Ding FC, et al. Change of asphaltene and resin properties after catalytic aquathermolysis. *Pet Sci*. 2009;6(2):194–200. doi:10.1007/s12182-009-0031-y.
- Zhao DW, Wang J, Gates ID, et al. Thermal recovery strategies for thin heavy oil reservoirs. *Fuel*. 2014;117:431–41. doi:10.1016/j.fuel.2013.09.023.
- Zhao XF, Tan XH, Liu YJ, et al. Behavior of an oil-soluble catalyst for aquathermolysis of heavy oil. *Ind Catal*. 2008;11:31–4. doi:10.3969/j.ssn.1008-1143.